

Common signatures of statistical Coulomb fragmentation of highly excited nuclei and phase transitions in confined microcanonical systems

J. Tőke and W. U. Schröder

Departments of Chemistry and Physics, University of Rochester, Rochester, New York 14627, USA

(Received 23 February 2009; published 29 June 2009)

Characteristic signatures of statistical Coulomb fragmentation of highly excited nuclear systems are analyzed. It is found that in many important aspects, they coincide with perceived signatures of phase transitions in confined hypothetical pseudomicrocanonical systems and, therefore, may give rise to an incorrect interpretation of certain experimental observations in terms of phase transitions occurring in nuclear matter. It is demonstrated that domains of negative heat capacity predicted by certain classes of pseudomicrocanonical model calculations for the immediate vicinity of phase transitions are artifacts of an unphysical truncation of the model phase space and that such domains disappear already with a very rudimentary enhancement of this phase space. Appearance of bimodality and of signatures of critical phenomena in Coulomb fragmentation is discussed.

DOI: [10.1103/PhysRevC.79.064622](https://doi.org/10.1103/PhysRevC.79.064622)

PACS number(s): 25.70.Gh, 24.60.Dr, 25.70.Jj, 25.70.Pq

I. INTRODUCTION

For over a quarter of century now, the observed process of disintegration of highly excited nuclear systems into multiple intermediate-mass fragments (IMF) has provided a strong driving force for research in the field of intermediate-energy heavy-ion reactions. This process, commonly called multifragmentation, has inspired both, theoretical speculations regarding its mechanism and experimental effort to map out its characteristics. Experimental observations point often to dynamical IMF production mechanisms, but they also reveal “robust” patterns commonly attributed to statistical production mechanisms [1]. While there appears to be a general consensus regarding the presence of a statistical component in the observed IMF yield, the standard equilibrium-statistical decay codes [2,3] with their gentle Boltzmann-like scaling of yields are not able to predict meaningful yields of intermediate-mass fragments (IMFs) heavier than lithium. The difficulty arises here from the fact that experimental yields show a significant departure from Boltzmann-like scaling with a fixed transition-state energy. Rather, single and multiple IMF production are seen to set in rapidly with excitation energy, in a fashion reminiscent of phase transitions, raising tempting prospects for experimental studies of phase transitions in microscopically small (nuclear) systems.

As a result of the difficulties encountered by standard equilibrium-statistical models to explain abundant statistical IMF production and to effectively parametrize some of the salient trends in the observed IMF yields, a number of models [4–9] have been proposed that supplement the traditional framework of statistical theory by incorporating either explicitly or implicitly ancillary (*ad hoc*) assumptions. The nature of these *ad hoc* assumptions is such that there appears to be no obvious way to justify them in the framework of known physical theory and that their only “validation” appears to be a satisfactory fit of resulting “predictions” to select experimental observations. Furthermore, these models describe mostly stationary *equilibrium* states, typically of spatially confined systems, without addressing the paramount issue of stability with respect to actual *decay* modes. The

relevance of such model calculations for nuclear matter is sometimes asserted by invoking the principle of universality, which is merely a heuristic notion. Similarly, although IMF yields predicted in these models [5,6,8] appear to exhibit patterns reminiscent of phase transitions, conclusions that nuclear multifragmentation is a manifestation of a nuclear liquid-gas phase transition are in fact unfounded hypotheticals. Nevertheless, in spite of an obvious lack of a sound theoretical foundation, over the years a paradigm or dogma has appeared in linking nuclear multifragmentation with nuclear phase transitions and “collateral” phenomena such as negative heat capacity, bimodality, or criticality.

To illustrate in more detail the point regarding the *ad hoc* nature of “mainstream” multifragmentation models, one notes that in the Copenhagen [5] and Berlin [6] multifragmentation codes, treated here as benchmarks, the model “nuclear” matter is tacitly taken to be infinitely *incompressible* in the liquid phase and infinitely *compressible* in the gaseous phase. Such a peculiar model equation of state (EOS) is not stated explicitly, but can be inferred from the fact that these models do not allow matter to undergo thermal expansion and set interaction energy to zero for the gas phase, regardless of matter density (including the ground-state density of nuclear matter). The equilibrium state assumed in these models is that of an ensemble of spherical objects that are continually scattering off each other and off the walls of a hypothetical spatial containment, the so-called freeze-out volume, while at the same time evaporating, reabsorbing, and exchanging nucleons and excitation energy among themselves. An important, but little noticed, fact is that, contrary to common beliefs, these models do not predict statistical breakup of the system at all in the sense the term “breakup” appears to suggest, i.e., as a fast single act. What they actually do predict is only that highly excited matter with the particular model EOS would time-asymptotically end up fragmented. It may do so plausibly by evaporating nucleons into the free space of the “freeze-out” volume, where these nucleons subsequently synthesize into intermediate-mass clusters or fragments. Obviously, the nature of these models is such that they cannot distinguish between a

physically single-act breakup and the more lengthy process of evaporation and nucleosynthesis.

The present work is part of a continued effort [10–18] to model the behavior of finite nuclear systems with diffuse surface domains within the framework of liquid drop and Fermi gas models and to construct a thermodynamical framework for understanding nuclear multifragmentation as a natural, fissionlike decay mode of highly excited compound nuclei, all while avoiding *ad hoc* assumptions of the kind discussed above. It is worth noting in this context that the standard statistical decay models [2,3] were designed for compound nuclei at low to moderate excitations, where particle evaporation and fission rates obey quite well Boltzmann scaling. At higher excitation energies, of the order of $E^*/A > 2\text{--}3$ MeV, physical phenomena of thermal expansion, reduction in surface tension, and growth of shape fluctuations can become important and alter nuclear decay patterns qualitatively.

Recently [12,15], it was shown that, when even a very rudimentary allowance is made for the surface entropy and thermal expansion of nuclear matter, the basic statistical scenario of asymmetric fission is quite sufficient to explain the large observed IMF yields and also to explain multifragmentation as a form of generalized fission associated with multifragment saddle shapes. In this scenario, an excited nucleus approaches a state of local thermodynamical equilibrium that is conceptually identical to that of a compound nucleus. The term “local” refers here to a finite volume in the phase space delimited by the hypersurface of transition states, i.e., states connecting to the open decay channels. In contrast to the “classical” low-energy compound nucleus, however, the system is now allowed to maximize its entropy by expanding thermally to corresponding equilibrium density and by exercising substantial shape fluctuations.

Obviously, equilibration of shape degrees of freedom is part of the overall equilibration process, where the system is “racing” for its survival against particle evaporation and other decay modes and where its “life expectancy” diminishes with increasing excitation energy as the decay time scales shorten. How far the system is able to advance on its path toward equilibrium depends critically on the latter time scales. The general assumption here, as in “classical” compound nucleus model, is that the degree of equilibration actually reached is sufficient to justify application of equilibrium statistical thermodynamics as a meaningful approximation. It is also worth noting in this context that the equilibration process sets in already as first amounts of excitation energy are supplied to the system by the collision dynamics and not, as some models (e.g., Ref. [4]) assume, after all of the excitation energy had been supplied. “Fortunately,” in the (doomed) race for survival mentioned above, the system is assisted by a peculiar feedback such that thermal expansion and excitation of shape degrees of freedom cause nuclear temperature to decrease (expansion cooling), thus extending particle evaporation time scales [13]. It is worth noting that such a feedback mechanism is an expected manifestation of Le Chatelier’s principle, where the system responds to the supplied excitation energy in a way (expansion plus fluctuations) that opposes the direct result of this supply—increase in temperature. As the system, on its way

toward equilibrium, reaches randomly a particular binary or more complex saddle configuration, it is driven toward scission by Coulomb and/or centrifugal forces resulting in observed fragment yields.

For the purpose of the following discussion, the decay scenario described above is named Coulomb fragmentation, to reflect the crucial role of Coulomb forces in the ultimate *dynamical* breakup of the system into two or more individual fragments. In fact, this is the same scenario that is considered, e.g., by the statistical decay code GEMINI [3]. This code succeeds in describing quasisymmetric but not highly asymmetric binary fission, where the latter failure is attributable to an inadequate accounting, of thermal expansion of nuclei and of the role that the surface entropy plays in the process.

As was shown recently [15], asymmetric binary Coulomb fragmentation is described by equations that are largely equivalent to the parametrization used with the nuclear Fisher droplet model [19] to fit a large volume of experimental data. In addition, multiple Coulomb fragmentation is consistent with the numerical procedures used in the statistical multifragmentation codes SMM [5] and MMMC [6], providing an explanation for why these codes appear to agree with selected sets of experimental observations.

The present study shows for the first time that statistical Coulomb fragmentation of finite nuclei shares some prominent signatures with first- and second-order phase-transitions in spatially confined pseudomicrocanonical systems. Most notably, such a process sets in rather suddenly with excitation energy and in a “non-Boltzmannian” fashion and may also exhibit apparent negative heat capacity and bimodality. Furthermore, at sufficiently high excitation energies, where the surface tension vanishes, statistical Coulomb fragmentation may also be expected to exhibit signatures of criticality, where the outcome is decided by combinatorial factors only. In other words, a rapid onset of single and multiple IMF production, the bimodality of select distributions, an apparent negative heat capacity and the “rule” of power law, are all consistent with and occur naturally in Coulomb fragmentation of hot nuclei. These findings challenge the concept of multifragmentation as a manifestation of a liquid-gas phase transitions in finite nuclear systems and favor the simpler, more plausible Coulomb fragmentation scenario.

The following Sec. II briefly reintroduces the schematic model of Ref. [11] and demonstrates that the two phenomena, second-order phase transitions in confined pseudo-microcanonical systems and statistical Coulomb fragmentation, are described by a common mathematical formalism. Both are manifestations of the crossing of relevant partition functions on the excitation energy scale.

In Sec. III, the significance of experimental trends in fragment productions is discussed in terms of Coulomb fragmentation. Here, the possibilities for observing signatures of first- and second-order phase transitions, as well as criticality are assessed.

Section IV offers an extended discussion and a summary. This section stresses the importance of the diffuse surface domain for nuclear stability and provides a tentative road-map for a further exploration of Coulomb fragmentation.

II. MODELING OF PHASE TRANSITIONS IN CONFINED PSEUDO-MICROCANONICAL SYSTEMS AND OF STATISTICAL COULOMB FRAGMENTATION

For the purpose of this study, a schematic model [11] is considered that emulates essentials of the (benchmark) pseudomicrocanonical models SMM [5] and MMMC [6], as far as phase transitions are concerned, but at the same time allows one to model Coulomb fragmentation [15]. The model considers a finite amount of isoneutral Fermi matter that is allowed to assume two spatial configurations, a spherical mononucleus and a symmetric dinuclear configuration of two equal touching spheres. These two configurations are taken to represent either two distinct phases of a confined nuclear system or two spatial configurations of an open system. In the latter context, the dinuclear configuration represents a transition state (saddle) connecting to an open binary fragmentation channel. Importantly, this model accounts for the diffuse nuclear surface domain, including in the calculations both surface energy and entropy [12]. As demonstrated in Ref. [12], the diffuse surface domain has profound, qualitative effects on the evolution of the system with increasing excitation energy.

In the qualification of SMM [5], MMMC [6], and other models, the prefix “pseudo-” is used to stress the important fact that only a truncated phase space is numerically manageable in calculations for systems at the high excitation energies of interest here. Quite naturally, the same prefix applies to the model used in the present study. As shown further below, an incomplete accounting of phase space may have nontrivial, qualitative consequences specifically in domains of phase transitions. In fact, the omission of certain parts of phase space may well be responsible for apparent but false signatures of such transitions, such as the negative heat capacity and some forms of bimodality reported in the literature [1].

In what follows, a “phase” is defined as a macroscopically distinct state of the system. Accordingly, a phase transition is defined here as an event in which the most likely phase of the system changes, as the value of the control parameter changes. Of course, small systems fluctuate strongly between different phases, where the relative dwelling times are given by phase partition functions. Because the fundamental difference between the conventional first- and second-order phase transitions is that the former involve transfer of latent heat while the latter do not, the phase transitions considered here are “nominally” of second order.

The above definitions of phases and phase transitions are fully consistent with conventional thermodynamics, a fact that is reiterated here to enhance the clarity of a chain of arguments made further below. While for the sake of specificity, in what follows, reference is mostly made to phases and phase transitions, one should keep in mind that the same applies always to macroscopic configurations of an open system, as well.

Formally, the probability w_i of finding the system in a particular phase is given by the associated partition function,

$$w_i = \frac{Z_i}{\sum_k Z_k}. \quad (1)$$

For a microcanonical statistical ensemble, which is the ensemble most suitable for the description of isolated systems, partition functions for individual phases (phase partition functions) are expressed via the associated entropies S_i (phase entropies). Therefore,

$$w_i = \frac{e^{S_i}}{\sum_k e^{S_k}}. \quad (2)$$

With the above conventional definition of material phases, a phase transition occurs when the partition functions for different phases intersect, as the controlling parameter (such as the total energy or the temperature) is varied. This point is illustrated with the schematic pseudomicrocanonical model of Ref. [11], which permits just two distinct macroscopic states of an excited nuclear system, the mononuclear and the symmetric dinuclear configuration. In this case the pseudomicrocanonical weight functions $w_i(E^*)$ for the two configurations i are functions of the total excitation energy E^* of the system. They are related to the phase entropies S_m and S_d associated with mono- and dinuclear configurations, respectively. These are the formal entropies calculated for the system in either a pure mononuclear (subscript m) or a pure dinuclear (subscript d) configuration,

$$w_{m/d}(N, E, V) = e^{S_{m/d}(N, E, V)}. \quad (3)$$

Here, N is the number of particles in the system and V is the system volume, here taken to be constant. Because of the above simple microcanonical relationship between a weight function and the corresponding configurational entropy, a (second-order) phase transition will occur at a system energy of $E = E_{p.T.}$, where the entropy functions for the two configurations or phases cross, i.e., where $S_m(N, E_{p.T.}, V) = S_d(N, E_{p.T.}, V)$. Note that for canonical ensembles (constant particle number N , constant temperature T , and fixed volume V), the corresponding weight functions can be expressed in terms of the Helmholtz free energies A_i ,

$$w_{m/d}(N, T, V) = e^{-A_{m/d}(N, T, V)/T}. \quad (4)$$

Accordingly, for an isothermal-isobaric ensemble (constant values of N , temperature T , and pressure p) the weight functions are properly expressed in terms of the Gibbs free energies G_i

$$w_{m/d}(N, T, p) = e^{-G_{m/d}(N, T, p)/T}. \quad (5)$$

Obviously, for all three kinds of ensembles considered above, any crossing of the configurational weight functions for any two macroscopically distinct configurations (phases) occurs at that value of the control parameter (E for microcanonical ensembles, otherwise T) at which the corresponding pairs of thermodynamic state functions (S , A , or G) intersect. In the thermodynamical limit, such crossing of the relevant special thermodynamic state functions results in a “logarithmic singularity” in the relevant partition function such that the respective first derivatives of logarithms of these partition functions are discontinuous. This singularity is reflected in corresponding singularities of the various thermodynamical functions.

Using the Fermi gas model to calculate the level densities of the constituent spherical fragments, the conditional entropies

for the pseudomicrocanonical mono- and symmetric dinuclear configurations considered here can be written as

$$S_m(A, E^*) = 2\sqrt{a_m E^*} \quad (6)$$

and

$$S_d = 2\sqrt{a_d [E^* - (E_d^{\text{pot}} - E_m^{\text{pot}})]}. \quad (7)$$

In Eqs. (6) and (7), a_m and a_d are the level-density parameters (*little-a*) for mono- and dinuclear configurations, respectively, and E_m^{pot} and E_d^{pot} are the potential energies of these configurations. The level-density parameters for a realistic nuclear matter distribution with diffuse surface domain can be calculated using the Thomas-Fermi approximation. They can be expressed approximately [10] in terms of volume and surface contributions,

$$a_m = \frac{A}{14} (1 + 4A^{-1/3}) \text{ MeV}^{-1} \quad (8)$$

and

$$a_d = 2 \frac{A}{28} \left[1 + \left(\frac{A}{2} \right)^{-1/3} \right] \text{ MeV}^{-1}. \quad (9)$$

The potential energies E_d and E_m for di- and mononuclear configurations can be calculated from the liquid drop model [20] such that their difference is equal to the difference in the sums of surface and Coulomb energies for the two configurations

$$E_d - E_m = c_{\text{Surf}} (F_2^d - 1) A^{2/3} + \Delta E_{\text{Coul}}. \quad (10)$$

Here c_{Surf} is the surface energy coefficient and $F_2^d = 2^{1/3}$ is the ratio of the surface area of the symmetric dinucleus to that of a single sphere of the same volume. The Coulomb term is left out for the purpose of this study.

Accounting for a surface specific contribution to the level-density parameter is essential for the present study. In particular, it is crucial for developing a quantitative understanding of Coulomb fragmentation, both binary and multiple. This surface level-density term approximately accounts for the excess entropy per nucleon (surface entropy) contributed by the dilute matter in the diffuse surface domain, relative to that of the denser bulk matter. At elevated excitation energies this extra surface entropy becomes large enough to significantly enhance the chances for a system to populate configurations with large surface areas such as represented by the dinuclear phase of a confined system and the saddle configuration of an open system. The surface entropy is also directly responsible for an intersecting of the weight functions for different configurations at characteristic excitations [11] signaling a phase transition as defined above. This feature is illustrated in figures presented further below.

In Figs. 1 and 2 results are shown of model calculations for a two-configuration system allowing mono- and symmetric dinuclear configurations within the schematic formalism [11] discussed above. For the sake of an easier demonstration of the effects of the size of the system the Coulomb interaction was left out in these particular calculations.

The top panel of Fig. 1 illustrates the intersecting of the entropy functions for the two (mono- and di-) model phases at

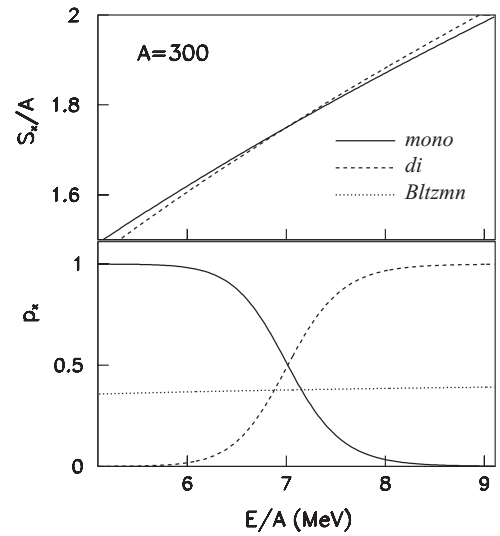


FIG. 1. Functional dependence of entropies (top panel) and relative population probabilities (bottom panel) for mono- and dinuclear phases, solid and dashed lines, respectively) on excitation energy per nucleon exhibiting a crossing at approximately $E/A = 7$ MeV. The dotted line in bottom panel illustrates Boltzmann-like behavior for a hypothetical dinuclear phase with 4 MeV of potential energy and with no gain in surface entropy.

a “crossover” excitation energy of $E/A \approx 7$ MeV, which also signifies the crossing of the corresponding weight functions for the two configurations. The calculations are for a system of $A = 300$ nucleons.

The bottom panel of Fig. 1 illustrates the way in which the relative population probabilities of the two phases of interest evolve with increasing excitation energy. As seen in this panel, at low excitations, where $S_m > S_d$, the system dwells dominantly in the mononuclear configuration or phase (solid line). As the excitation energy increases and approaches the

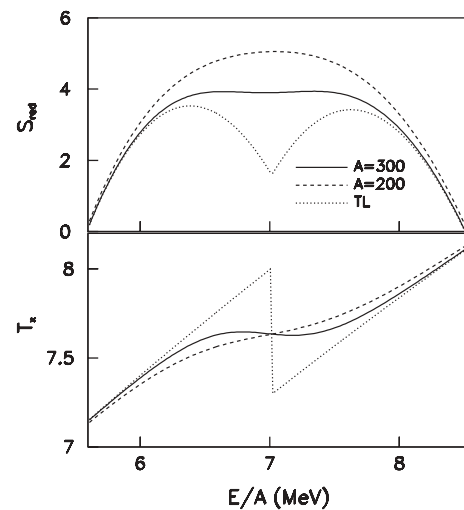


FIG. 2. Reduced entropy (top panel) and system temperature (bottom panel) vs. excitation energy per nucleon for the two-phase system of mono- and dinuclear configurations and three sizes of the system: thermodynamic limit (TL), “large” with $A = 300$, and “intermediate” with $A = 200$ (see text).

crossing point, the system fluctuates more frequently away from the mononuclear configuration into the dinuclear domain (dashed line). In the vicinity of the “crossover” energy, the two phases coexist, but not in the sense of conventional first-order phase transitions for macroscopic systems, where, e.g., finite amounts of liquid and gas are simultaneously present in a given volume. Rather, the system continually jumps from one phase to the other (at no cost in latent heat) but at any instant in time is either in one or in the other pure macroscopic state or phase. At higher excitation energies, beyond the crossover energy, the system is found dominantly in the dinuclear state or phase. Notable in Fig. 1, bottom panel is the rapidity with which the dinuclear phase sets in, as excitation energy is increased. It should be kept in mind that the same “phase-transition-like” scaling with E/A applies to the population probability of the fragmentation saddle configuration as compared, e.g., with the population of (compact) particle emission transition states. Such a “phase-transition-like” scaling is in stark contrast with the Boltzmann-like scaling illustrated in the bottom panel of Fig. 1 by a dotted line. The latter is calculated for a hypothetical configuration with just 4 MeV of potential energy and with no gain in surface entropy with respect to the mononuclear configuration. Note that the population probability of this hypothetical configuration approaches asymptotically the probability of the mononuclear configuration, but never “overtakes” it.

The thermodynamics of phase transitions in the present schematic model can be further explored by studying the evolution of the system entropy (as opposed to phase entropies) with increasing excitation energy. This system entropy is given by the logarithm of the microcanonical partition sum

$$S_{[m,d]}(E) = \ln[e^{S_m(E)} + e^{S_d(E)}], \quad (11)$$

where $S_m(E)$ and $S_d(E)$ are phase entropies for the mono- and dinuclear configurations. For a better demonstration of important mathematical properties of the system entropy $S_{[m,d]}$, a reduced entropy is defined such that a linear function is subtracted from the former that makes the latter zero at the boundaries of the energy region of interest. Importantly, the subtraction of a linear function preserves the second derivative and thus does not affect properties of interest here, such as convexity or concavity.

A reduced entropy function per nucleon (multiplied by 1000) for the ensemble considered here and the corresponding caloric curves are illustrated in Fig. 2 for three different sizes of the system: infinite (TL: $A \rightarrow \infty$), large ($A = 300$), and intermediate ($A = 200$). The calculations were performed according to Eqs. (6), (7), and (11) for the case of $A = 300$. To preserve the location of the crossing point of the entropy functions and to isolate the effect of the overall system size from that of the relative size of the surface domain, the entropy for the case of $A = 200$ was calculated using Eq. (11), with S_m and S_d obtained by renormalizing by a factor of 200/300 the entropies calculated for the system of $A = 300$. In the same spirit, the data for the thermodynamic limit were obtained from calculations for the $A = 300$ system by taking the mononuclear entropy function for excitation energies below the crossover point and the dinuclear entropy function above this point. Obviously, in the true thermodynamic limit, not

only do fluctuations vanish but also any surface effects must vanish.

As seen in the top panel of Fig. 2, in the thermodynamic limit the reduced entropy (and hence the model entropy) features a singularity at the crossing of entropy functions around $E/A = 7$ MeV but remains always a concave function of the energy. Correspondingly, caloric equation of state features a singularity in the form of a jump (bottom panel). Fluctuations present in finite systems make the entropy differentiable at all energies, although larger systems with smaller fluctuations exhibit a qualitatively different behavior. As seen also in the top panel of Fig. 2, in the “large” system ($A = 300$), a convex domain or “convex intruder” persists as a telltale remnant of the kink present in the case of the thermodynamic limit. This convex intruder maps then onto the caloric equation of state as a domain of negative heat capacity (bottom panel). The more “robust” fluctuations present in the “intermediate-size” system ($A = 200$) further “heal” the entropy function, which is now strictly concave. Accordingly, the heat capacity is always positive (bottom panel). The thermodynamic temperatures plotted in the bottom panel of Fig. 2 are calculated according to the standard microcanonical expression for the average temperature

$$T^{-1} = \beta = \frac{dS}{dE}. \quad (12)$$

A. Origins of an apparent negative heat capacity

In principle, irregularities or nonmonotonicities in the caloric curve $T(E)$ appear possible in the phase-transition domain of physical systems. However, to prove in numerical modeling the presence of a negative heat capacity in such a domain is exceedingly difficult, if not impossible. This is so because it is obviously technically impossible to include in the model calculations explicitly all energetically allowed microstates of a physical system. Neither is it feasible to include all possible macroscopic configurations. Therefore, it is impossible to deduce the true entropy function and the corresponding true microcanonical temperature. Actual numerical simulations can address only finite subspaces of an untractably large true microcanonical phase space. Therefore, in such simulation calculations only apparent or pseudothermodynamic potentials and functions are evaluated and not the true functions. It is therefore impossible to tell whether any particular fine (as opposed to gross or average) trend in an apparent thermodynamical quantity deduced for a numerical model system reflects its true thermodynamical counterpart in a physical system. Specifically, it is impossible to predict fine trends in thermodynamical functions for physical systems with phase-space-truncated numerical calculations on which models such as SMM [5], MMMC [6], and lattice gas models [8] are based. Concerning reports of apparent negative heat capacities for physical systems, for example, it is demonstrated further below that the exclusion of certain classes of microstates from experimental observation may result in a corresponding artifact.

In evaluating such apparent caloric phenomena, one notes first that it is physically impossible for a nuclear system to populate just two distinctly different macroscopic spatial

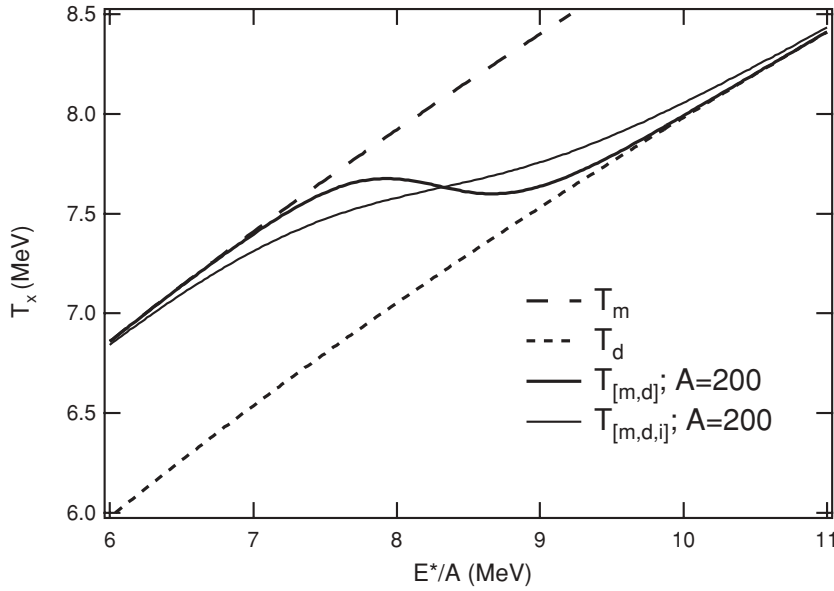


FIG. 3. The “healing” effect of an interphase configuration on the apparent caloric curve for the two-phase system of mono- and dinuclear configurations for a $A = 200$ system.

configurations, such as the ones (m and d) used in the schematic model introduced previously, without also populating the entire continuum of intermediate macrostates, those “connecting” the two limiting spatial distributions. In fact, physical systems must be able to follow continuous pathways connecting any number of macroscopic spatial configurations. In the present context, it is impossible for a spherical mononucleus to jump to a symmetric dinuclear configuration without passing through a continuous sequence of intermediate states of various intermediate deformations. Similar considerations apply to the configuration spaces considered by SMM [5], MMMC [6], and lattice gas [8] models. Importantly, the intermediate macroscopic configurations have a noticeable influence on the apparent trends of thermodynamic functions exactly in the domain of phase transitions, i.e., where the weight functions for the phases (configurations) of interest cross. This is so, because the weight functions of the intermediate configurations must intersect the weight functions for the phases of interest in the immediate vicinity of their crossing. Therefore, the intermediate configurations make a noticeable contribution to the overall partition function selectively only in this domain. Consequently, exclusion of any of these intermediate configurations depletes the model entropy locally (on the energy scale) and may give rise to a false convex intruder in the entropy function $S(E)$. Effects of such false convex intruder propagate to other thermodynamic functions and representations of thermodynamic observables. In particular, a false intruder results in a caloric curve featuring a domain of apparent negative heat capacities. This rather trivial mechanism of generating *unphysical* negative heat capacity in truncated-space microcanonical calculations is illustrated in more detail in Fig. 3.

Figure 3 illustrates effects of an exclusion of intermediate macrostates by considering the effect associated with just one extra deformed configuration intermediate between the two limits of spherical mono- and deformed dinuclear (“base”) configurations. The assumed interphase configuration corresponds to a deformation parameter of $F_2 = 1.13$, where F_2 is

the ratio of the surface area of a configuration to the surface area of a sphere of equal volume. This parameter value is halfway between the respective values for spherical mononuclear ($F_2 = 1$) and dinuclear ($F_2 = 2^{1/3}$) configurations. As seen already in Fig. 2, the apparent entropy $S_{[m,d]}(E)$ for a system including only these two base configurations (m and d) exhibits a convex intruder in the vicinity of the crossing point of the phase entropy functions $S_m(E)$ and $S_d(E)$. The caloric curve $T_{[m,d]}(E)$ deduced for a hypothetical system with such a drastically truncated phase space features a negative heat capacity in the vicinity of this crossing (cf. Fig. 2). As seen in Fig. 3, restoring the previously neglected additional intermediate interphase (i) configuration with a deformation parameter of $F_2^i = 0.5(F_2^m + F_2^d)$ changes the apparent caloric curve $T_{[m,d,i]}(E)$ qualitatively, causing the domain of apparent negative heat capacity to disappear. The mechanism of elimination of this domain can be understood in more detail from Fig. 4

The top panel of Fig. 4 illustrates the sequential crossing of entropy functions for mononuclear (solid line), intermediate (dashes), and dinuclear (dotted line) phases in a three-phase system. The entropy functions are plotted relative to that for the mononuclear configuration to enhance the view. At low excitations, mononuclear configuration dominates. As the excitation energy increases, first the intermediate configuration “catches up” with the mononuclear phase, becoming the dominant phase around $E/A \approx 7$ MeV. Subsequently, the dinuclear phase “catches up” with the intermediate one, becoming dominant around $E/A \approx 7.3$ MeV. As seen in the middle panel of Fig. 4, the “interphase” configuration (i) plays a noticeable role selectively only in the vicinity of the crossover energy of the weight functions w_m and w_d for the two phases considered. Accordingly, as seen in the bottom panel of Fig. 4, it contributes to the overall apparent entropy only in the energy region of the phase transition but not much beyond it. It is this additional entropy component, which is not accounted for in the truncated two-phase phase space, that restores the overall concavity of the entropy as a function of energy. This

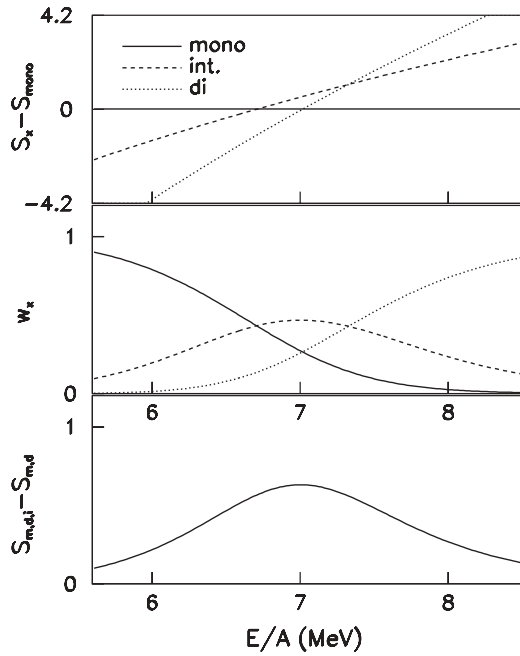


FIG. 4. Crossing of relative phase entropy functions (top panel) and phase weight functions (middle panel) for three macroscopic configurations, mono- and dinuclear (subscripts m and d) and intermediate (i) as functions of energy. The bottom panel illustrates the extra system entropy resulting from the presence of the intermediate phase i .

“healing” is achieved by a slight reduction in the system temperature caused by the ascending slope and a slight increase caused by the descending slope of the intermediate entropy function, consistent with the definition of temperature as $T^{-1} = \partial S / \partial E$.

The present schematic calculation demonstrates that, in the vicinity of an anticipated phase transition (crossing of weight functions), apparent thermodynamic quantities behave qualitatively differently when certain classes of valid macrostates are excluded from the numerical calculations or from observation. As it is practically impossible to guarantee that all relevant states are included in any realistic model description, model calculations do not provide a sound foundation for conclusions regarding fine trends in thermodynamical functions. This is especially true in the vicinity of phase transitions.

B. Apparent bimodality

Recently, suggestions have been made Refs. [21,22] that the bimodality of certain distributions or of thermodynamic functions represents a robust signature of a nuclear liquid-gas phase transitions. In this context, one is immediately reminded of examples of bimodal distributions that are associated with other phenomena. For example, the statistical competition of Coulomb fragmentation or fission with particle evaporation results naturally in bimodal distributions of various observables. In the schematic model discussed previously, postevaporation fragment mass distribution are bimodal for excitation energies close to the crossover energy, where the entropy functions for mononuclear configuration $[S_m(E^*)]$ and dinuclear saddle

configuration $[S_d(E^*)]$ intersect. In this case, one peak in the mass distribution represents the massive evaporation residues of the primary mononuclear product, while the second peak just below one-half of the total system mass represents the evaporation residues of the two, nearly symmetric fragments produced in the primary Coulomb fragmentation process. One may also expect a bimodal temperature distribution, with a lower average temperature for the fragmentation channel. This kind of bimodality is in fact well known from fission studies. Evidently, bimodality is not an exclusive signature of phase transitions and its experimental observation can therefore not be taken as proof that such a transition actually occurs in excited nuclei.

C. First-order phase transitions in small systems with truncated phase space

Quite generally, first-order phase transitions in small confined microcanonical systems can be viewed as a rapid succession along the energy axis of crossings of weight or entropy functions for a series of macroscopic configurations or phases, e.g., those associated with a successively increasing number of gas particles. In the aggregate, a succession of such second-order phase transitions has the appearance of a conventional first-order phase transition. In this case, the latent heat conventionally associated with first-order transitions is represented here by the difference in excitation energies between adjacent crossing points of phase entropy functions. As discussed further above, at crossings, phase transitions occur without infusion of energy from an external source, i.e., with zero latent heat. To illustrate the above point, a sequence of crossings of entropy functions for 20 configurations, including the mononuclear, dinuclear, and 18 intermediate with uniformly spaced deformation (surface area) parameters F_2 , is illustrated in Fig. 5. As discussed further below, the

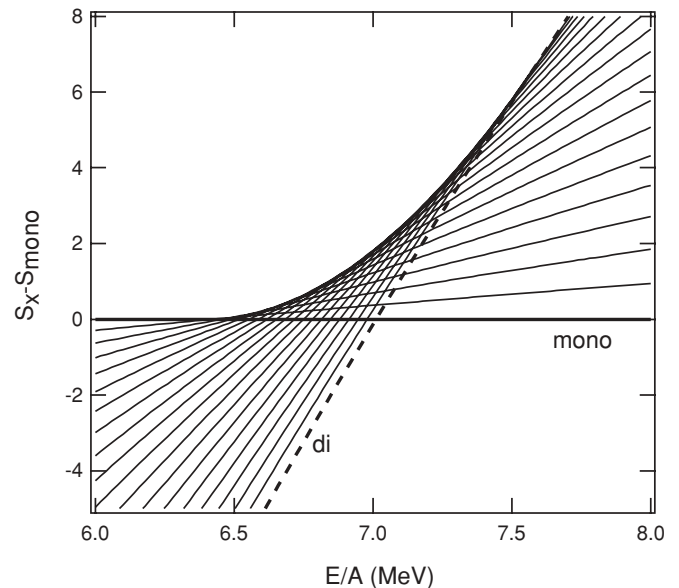


FIG. 5. Crossing of relative phase entropy functions for 20 macro-configurations (phases) with surface area parameters F_2 increasing from 1 (mono-) to $2^{1/3}$ (di-) in 20 equal steps.

sequence seen in Fig. 5 may be viewed as representing a first-order phase transition of matter from the dense bulk to the less dense surface domain.

In actual (small) nuclear systems, the energy intervals between the consecutive crossings (the apparent latent heat) may fluctuate significantly, for example, due to pairing or isospin effects. A scenario of successive second-order phase transitions accommodates such variations naturally and offers therefore a more direct access to the underlying transitional phenomena than one based on the corresponding picture of conventional first-order transition.

It is worth noting that in the SMM and MMMC models an otherwise dominant population of the gas phase is suppressed by an *ad hoc* resetting of the gas interaction energy to zero at any density. At the same time, these calculations artificially enhance the relative weights of multifragment configurations by an *ad hoc* setting of the nuclear incompressibility modulus to infinity. As a result, in these models, the crossings of the overestimated weight functions for many multifragment configurations occur in the same excitation energy domain where crossings would occur between entropy functions for different liquid-gas compositions, obscuring possibly a true first-order liquid-gas transition. It is of interest to have SMM- or MMMC-type calculations performed for “numerical” matter with a more realistic effective EOS to see whether such more realistic model matter would still be predicted to “clusterize” (via evaporation and nucleosynthesis) into various sets of IMFs plus relatively few free nucleons floating in a “freeze-out” volume. Alternatively, and more likely, such more realistic matter would end up as a large, thermally expanded liquid residue surrounded by a small amount of gas of interacting nucleons. However, such interest is purely academic, as it is not possible to confine a highly excited nuclear system to a fixed spatial volume, as would be required to confirm or falsify improved model predictions.

III. EXPERIMENTAL PHASE-TRANSITION-LIKE SIGNATURES IN COULOMB FRAGMENTATION

As discussed briefly further above, Coulomb fragmentation is a process similar to binary fission but generalized to arbitrary saddle shapes, including multifragment shapes [15]. The process can be described approximately in terms of microcanonical thermodynamics of an excited nuclear system, which surface tension confines transiently to a finite domain of $6A$ -dimensional (A is the mass number) phase space or the system phase space. This domain is delimited by a hypersurface in phase space that includes all possible transition states, i.e., those defined by particle evaporation barriers or thresholds, as well as the complete set of (multi-)fragmentation saddle configurations. To achieve maximum entropy, microcanonical equilibrium thermodynamics requires the system to explore all energetically allowed microstates with equal *a priori* probability. In the course of such an “exploration” and before it is completed, the system reaches eventually a microstate on the hypersurface of transition states that is connected to an open decay channel. If this happens to be a particle emission channel, a particle escapes while the residual system

evolves toward a new equilibrium characterized by accordingly reduced energy and particle numbers. Depending on the degree of the equilibration reached, the just-emitted particle is viewed as an evaporated or as a pre-equilibrium ejectile. However, if the transition state represents a fragmentation saddle configuration, the system is driven toward scission, all the while continuing its exploration of the accessible phase space. The basic macroscopic phenomena associated with equilibration are thermal expansion and thermal shape fluctuations. The latter are responsible for Coulomb fragmentation, i.e., for bringing the system occasionally to a particular saddle configuration from which it is dynamically driven apart by Coulomb forces. The above picture is essentially identical to a compound nuclear fission scenario and to the IMF production scenario adopted in statistical decay models. A novel observation made only recently [12] is that extra entropy associated with the diffuse surface domain plays a critical role in facilitating large and complex shape fluctuations.

A. Signatures of second-order phase transitions

The probability for an excited nuclear system to arrive at a particular transition-state configuration is given by a respective weight function identical to the one discussed further above in the context of phase transitions of confined systems. The weight functions for various transition-state configurations, given by Eq. (3), intersect at different, characteristic excitation energies. Because compact transition-states configurations are characterized by low potential energies, their entropy functions “take off” already at low excitation energies that, however, are insufficient for supporting higher potential energies associated with more deformed transition-state configurations. However, when with increasing excitation energy the entropy functions for deformed configurations eventually do “take off,” they grow at a rate superior to that for compact configurations. As a result, the entropy (weight) functions for different fragmentation channels cross and leave signatures reminiscent of second-order phase transitions.

It is worth noting that the observation of Coulomb fragmentation phenomena is subject to an inherent experimental filter that allows only the saddle configurations to pass but not all those configurations that did not quite “make it” to the saddle, i.e., configurations intermediate between the deformed saddle and the spherical reference configurations. However, to extract the true, and not just some apparent, values of the interesting thermodynamical parameters from experimental Coulomb fragmentation data from comparisons with theoretical simulations, such simulations need to include also the experimentally “invisible” configurations in the model space. To reiterate a statement made previously, it is virtually impossible to guarantee that deduced fine trends such as an apparent negative heat capacity are not simply artifacts resulting from the neglect of relevant configurations in the model phase space.

In view of the fact that reasonably sized systems have a large number of possible saddle shapes and corresponding crossings of the respective weight functions, one may wonder if, and under what circumstances, irregularities show up in the

apparent trends in thermodynamic quantities inferred from a cursory sampling via Coulomb fragmentation channels. Obviously, crossing points of the configurational weight functions are not distributed uniformly in energy. Rather, their distribution is expected to exhibit statistical fluctuations, including some local purely statistical bunchings. Sufficiently strong bunchings of crossing points along the excitation energy may show up as irregularities in an apparent caloric curve and perhaps even simulate a negative heat capacity. Such irregularities, however, should not be taken to signal phase transitions or transitions from one preferred individual fragmentation channel to another. Rather, such phenomena reflect statistical fluctuations in the distribution of crossing points in a fashion reminiscent of Ericson fluctuations [23] in compound nucleus decay at low excitations.

B. Signatures of first-order phase transitions and criticality

An instructive view on first-order phase transitions in finite nuclei can be obtained with the conventional definition of phases as referring to parts of the system, which allows one to consider one part of the system being in one phase (liquid) and the other part in a different phase (gas). In this approach, as was pointed out in Ref. [15], an excited nucleus is inherently a two-phase system, consisting of liquid quasiuniform bulk matter and diluted surface-domain matter. Obviously, these two phases are characterized by different densities, energies per nucleon, heat capacities, and even pressures.

With increasing excitation energy, in a quest for maximum entropy, the system seeks out an optimum macroscopic configuration with increased effective level-density parameter but at the cost of also increased potential energy. Note that quite generally, an increase in level-density parameter signifies a corresponding reduction in correlations: spatial, but also pairing and shell correlations. An obvious way to achieve maximum entropy leads through thermal expansion [12]. The other way leads through a transfer of matter from the spatially more correlated bulk to the less correlated surface domain, in what may be viewed as a true first-order liquid-gas phase transition. Such transfer is effected at the cost of increased potential energy in two distinctly different ways. First, the surface area and diffuseness will increase with increasing excitation energy. Second, and more importantly from the experimental point of view, thermal shape fluctuations grow in size with increasing excitation energy allowing one to experimentally probe their reaching of transition state deformations.

The presence of such a first-order, bulk-to-surface phase transition manifests itself in the Coulomb fragmentation excitation function as a fast succession of crossings of weight functions for fragmentation saddle configurations with successively increasing surface areas (see Fig. 5). This is a true conventional first-order liquid (bulk)-gas (surface) phase transition with latent heat represented by the amount of energy needed to cause transfer of a certain amount of nuclear matter from bulk to surface domain. With increasing excitation energy, the individual configuration entropy functions eventually

converge at a critical excitation energy, where the surface tension vanishes. As a result of this convergence, the probabilities of observing experimentally various multifragment configurations will be governed by combinatorial principles only, resulting in a power-law distribution of fragment masses and, consequently, in an appearance of signatures of criticality.

While it is not obvious what can be learned from discussing Coulomb fragmentation in the framework of first-order phase transitions, it appears likely that experimental trends and patterns of this phenomenon reflect primarily properties of the diluted, nonuniform nuclear surface matter. Therefore, a better understanding of fragmentation properties may help to detail the mapping of the EOS of moderately diluted nuclear matter, including its isospin dependence.

IV. DISCUSSION AND SUMMARY

It appears rather obvious that trends in apparent thermodynamical quantities modeled in numerical simulations of nuclear systems that sample only a fraction of the micro-canonical or canonical phase space do not accurately represent corresponding trends in their actual physical counterparts. This observation poses the question of whether such model trends reflect at least qualitatively the correct underlying physics and, conversely, under what circumstances predicted model trends in apparent quantities may even be qualitatively misleading. The present study demonstrates that qualitative discrepancies between physical processes and model interpretations are likely to occur for phenomena involving phase transitions, the very focus of many numerical modeling attempts. The numerical examples discussed above show that an omission of macroscopic configurations intermediate between those associated with different phases depletes the partition function selectively exactly in the excitation energy domain of interest but not much beyond it. As a result of such a depletion, one observes a deficit in apparent entropy (“convex intruder”) and an apparent or false negative heat capacity in the model calculations. No such deficit would be present in a calculation performed with a more complete phase space and a proper modeling of the containment vessel consistent with the second law of thermodynamics.

While modeling of a confined system is of purely academic interest, modeling the decay modes of excited nuclear systems is of practical importance. This latter venture aims at a deeper understanding of experimental observations rather than just parameterizing them. For the first time, the present study demonstrates that Coulomb fragmentation exhibits signatures deceptively similar to those of phase transitions in confined systems. Both sets of signatures are understood to reflect crossings of respective weight functions with increasing system excitation. Hence, this work offers a plausible explanation why Coulomb fragmentation can easily be mistaken for a nuclear phase transition in a confined system, a transition of either first or second order. It is also important to note that, not only in theoretical modeling but also in measurements of binary or multifragment decay, only a fraction of the relevant underlying phase space is sampled. Sampled are only

saddle-point configurations but none of the “intermediate” presaddle configurations. Therefore, also experimentally, one can determine directly only apparent thermodynamic quantities and their trends but not the trends in the true thermodynamic quantities describing the highly excited nuclear systems. A more accurate determination of trends has to rely on a comparison with simulations admitting a representative, sufficiently large subspace of the full configuration space.

Because of the large number of possible saddle configurations in reasonably sized systems and because of thermal fluctuations, it is unlikely for any single second-order “phase” transition between two distinct saddle configurations to leave a distinct and unambiguous experimental “fingerprint.” More likely, phase-transition-like signatures are observable in Coulomb fragmentation when random, statistical “bunching” of the crossing points of weight functions for different saddle configurations occurs at certain excitation energies. Such statistical fluctuations could result in observable irregularities, e.g., on caloric curves, somewhat reminiscent of Ericson fluctuations [23] in compound nucleus decay.

While it is not yet clear, what there is to be learned from the irregularities of apparent thermodynamic quantities extracted from nuclear fragmentation data, it is clear that an analysis of experimental data in terms of Coulomb fragmentation (generalized fission) has important implications for an understanding of properties and behavior of the surface domain of excited nuclei. In particular, such data may allow one to probe specifically the nuclear EOS of the diluted surface domain matter and, separately, also that of bulk nuclear matter diluted through thermal expansion. It is rather obvious from the lessons of compound nuclear fission that the stability of nuclear systems against fragmentation depends critically on the presence and the properties of a diffuse surface domain. As has been pointed out in Ref. [15] and further above, because of the differences in average density, binding energy, and level-density parameter between bulk and surface matter, finite nuclei are inherently two-phase systems. As the excitation energy of such a two-phase system is raised, matter is transferred from the bulk to the surface domain, which can be viewed as a true first-order liquid-gas phase transition. It is also natural to expect that, at high excitation energies, the surface tension generated by the density gradient in the surface domain will vanish and give rise to critical phenomena.

The signatures of Coulomb fragmentation can be probed experimentally in greater detail by studying excitation functions for individual fragmentation channels. Because the process appears to be controlled by the manner in which weight functions for various multifragment saddle shapes cross in succession, the yield for individual fragmentation channels is expected to exhibit a rise and fall with increasing excitation energy. (See Fig. 4, middle, Gaussian-like curve.) This may potentially open a completely new venue of experimental exploration of Coulomb fragmentation: spectroscopy of multifragment saddle configuration, where the excitation functions for various channels are studied, e.g., as functions of fragment sizes and isospins. Furthermore, it may be possible to use the location

of the peaks in various yields on the energy scale as a measure of excitation energy, i.e., as a tool of calorimetry of highly excited nuclei. Also, there must be situations, where two or more weight functions run quasiparallel avoiding each other but crossing some other weight functions. This effect will give rise to gentle Boltzmann-like scalings for some relative yields embedded in phase-transition-like scalings of some other yields. This situation may arise when two saddle shapes differ in isospin but not so much in surface area, leading to isoscaling.

With the above experimental opportunities in mind, a more coordinated theoretical effort appears warranted aiming to achieve a better quantitative understanding of the evolution of the properties of the surface domain with excitation energy [17,18] and other variables. To understand nuclear dynamics on a deeper level, it is important to assess the morphing of quasisymmetric binary fission first into asymmetric binary Coulomb fragmentation and then into multiple fragmentation. Such an effort would also advance thermodynamic theory of small open quantal systems inherently endowed with diffuse surface domains—a valuable goal in its own merits.

Finally, it is worth noting that, while the physics underlying the present schematic model differs conceptually from that reflected implicitly in the “benchmark” multifragmentation models SMM [5] and MMMC [6], the formal basis of all three models is the same [15]. It is expressed in the fact that more fragmented (i.e., less correlated) spatial configurations show higher entropy production rates (larger effective level density parameter a) and thus are able to “catch” up in terms of entropy (as excitation energy is increased) with more correlated but less fragmented configurations. In the present model, the extra *catch-up* entropy is produced for fragmented configurations due to their larger total surface domain. In SMM [5] and MMMC [6] models, however, extra entropy comes from the implicit thermal motion of spherical constituents of fragmented state within a hypothetical *oversize* confinement vessel—named as “freeze-out” volume. By adjusting the volume of this latter invisible vessel, one fine-tunes the magnitude of the extra entropy such that these models may ultimately appear to provide fits to selected experimental data. It is interesting to note that when moderately time averaged, such thermal motion of the spherical fragments produces an effective matter distribution that emulates the diffuseness of the surface domain of the actual matter distribution and emulates also complex multifragment saddle geometries. Consequently, to a good extent, the extra entropy generated by the fragment thermal motion is equivalent to the entropy due to the diffuse surface domain of the matter distribution. In fact, it is the latter observation that has inspired the present effort of exploring the role of the surface diffuseness in facilitating fragmentation of highly excited nuclear systems.

ACKNOWLEDGMENT

This work was supported by the US Department of Energy Grant No. DE-FG02-88ER40414.

- [1] B. Borderie, J. Frankland, A. Pagano, S. Pirrone, and F. Rizzo, eds., *Proceedings of the IWM2007 International Workshop on Multifragmentation and Related Topics* (Società Italiana di Fisica, Bologna, Italy, 2008).
- [2] A. Gavron, Phys. Rev. C **21**, 230 (1980).
- [3] R. J. Charity *et al.*, Computer code GEMINI, Nucl. Phys. **A483**, 371 (1988).
- [4] W. A. Friedman, Phys. Rev. Lett. **60**, 2125 (1988).
- [5] J. P. Bondorf *et al.*, Phys. Rep. **257**, 133 (1995).
- [6] D. H. E. Gross, Phys. Rep. **279**, 119 (1997).
- [7] M. E. Fisher, Physics (N.Y.) **3**, 255 (1967).
- [8] J. Pan and S. D. Gupta, Phys. Rev. C **51**, 1384 (1995).
- [9] W. Bauer, Phys. Rev. C **38**, 1297 (1988).
- [10] J. Töke and W. J. Swiatecki, Nucl. Phys. **A372**, 141 (1981).
- [11] J. Töke and W. U. Schröder, Phys. Rev. Lett. **82**, 5008 (1999).
- [12] J. Töke, J. Lu, and W. U. Schröder, Phys. Rev. C **67**, 034609 (2003).
- [13] J. Töke, L. Pieńkowski, L. Sobotka, M. Houck, and W. U. Schröder, Phys. Rev. C **72**, 031601(R) (2005).
- [14] J. Töke, J. Lu, and W. U. Schröder, Phys. Rev. C **67**, 044307 (2003).
- [15] J. Töke and W. U. Schröder, *Proceedings of the IWM2005 International Workshop on Multifragmentation and Related Topics* (Società Italiana di Fisica, Bologna, Italy, 2006), p. 379.
- [16] L. G. Sobotka, R. J. Charity, J. Töke, and W. U. Schröder, Phys. Rev. Lett. **93**, 132702 (2004).
- [17] L. G. Sobotka and R. J. Charity, Phys. Rev. C **73**, 014609 (2006).
- [18] C. Hoel, L. G. Sobotka, and R. J. Charity, Phys. Rev. C **75**, 017601 (2007).
- [19] J. B. Elliott, L. G. Moretto, L. Phair, G. J. Wozniak, L. Beaulieu, H. Breuer, R. G. Corteling, K. Kwiatkowski, T. Lefort, L. Pieńkowski *et al.*, Phys. Rev. Lett. **88**, 042701 (2002).
- [20] W. D. Myers and W. J. Swiatecki, Ann. Phys. **55**, 395 (1990).
- [21] D. Gross, *Microcanonical Thermodynamics: Phase Transitions in Small Systems* (World Scientific, Singapore, 2001), p. 379.
- [22] P. Chomaz and F. Gulminelli, Eur. Phys. J. A **30**, 317 (2006), and references therein.
- [23] T. Ericson, Phys. Rev. Lett. **5**, 430 (1960).